HTML ABSTRACT * LINKS

Nitrogen incorporation effects on gain properties of GaInNAs lasers: Experiment and theory

A. Thränhardt,[a] I. Kuznetsova, C. Schlichenmaier, and S. W. Koch
Fachbereich Physik, Philipps-Universität, Renthof 5, 35032 Marburg, Germany

L. Shterengas and G. Belenky
State University of New York at Stony Brook, Stony Brook, New York 11974-2350

J.-Y. Yeh and L. J. Mawst
University of Wisconsin-Madison, 1415 Engineering Drive, Madison, Wisconsin 53706-1691

N. Tansu
Center for Optical Technologies, Lehigh University, 7 Asa Drive, Bethlehem, Pennsylvania 18015

J. Hader and J. V. Moloney
Arizona Center for Mathematical Sciences and Optical Sciences Center, University of Arizona, Tucson, Arizona 85721

W. W. Chow
Sandia National Laboratories, Albuquerque, New Mexico 87185-0601

(Received 20 December 2004; accepted 4 April 2005; published online 12 May 2005)

Gain properties of GaInNAs lasers with different nitrogen concentrations in the quantum wells are investigated experimentally and theoretically. Whereas nitrogen incorporation induces appreciable modifications in the spectral extension and the carrier density dependence of the gain, it is found that the linewidth enhancement factor is reduced by inclusion of nitrogen, but basically unaffected by different nitrogen content due to the balancing between gain and index changes.
© *2005 American Institute of Physics*. [DOI: 10.1063/1.1929880]

The past few years have seen considerable activity in the development of dilute nitride semiconductor materials, motivated by the significant design flexibility of this material system. In particular, GaInNAs has the advantage of enabling GaAs-based laser structures (e.g., vertical cavity surface emissing laser, i.e., VCSELs) operating at telecommunication wavelengths.[1–3] This spectral range is particularly promising, since the currently used high-speed GaInAsP lasers suffer from the problems of poor heat conductivity and low-power capacity. Moreover, the fabrication of distributed Bragg reflectors (DBR) is more challenging because of the small refractive index difference achievable within the GaInAsP alloys. The mature GaAs/AlGaAs technology, on the other hand, allows for the growth of extremely high quality DBRs and VCSELs.[4]

Recent reports addressed various aspects of gain property modifications due to N incorporation into GaInNAs systems. Measurements of gain spectra and linewidth enhancement factors (LWEF) have been performed for a 1.3 μm GaInNAs structure.[5] The same quantities have been calculated in the GaInNAs material system using a free carrier[6–8] as well as a many-body theory.[9–12] Gain characteristics for 1.3-μm-wavelength GaInNAs, InGaAlAs, and InGaAsP,[13] as well as gain and threshold properties of lattice-matched $Ga_{1-y}In_yN_xAs_{1-x}$/GaAs for different values of x and y[10,14,15] have been investigated.

This letter extends the available information by addressing both threshold and modulation performance of GaInNAs systems. Central to our investigation is a detailed analysis of experimental results on the basis of a microscopic semiconductor theory, to provide an accurate estimation of carrier density (ρ), so that the excitation dependencies of gain and refractive index can be determined. The effect of N incorporation is studied by a systematic comparison of two similar lasers, where one contains an InGaAs gain region and the other a GaInNAs gain region.

For a realistic prediction of laser gain, we have found a microscopic inclusion of carrier–carrier and carrier–phonon scattering indispensable.[16] Additionally, the refractive index and thus the LWEF critically depends on the partial population of barrier states.[9] Inclusion of these effects allows us to critically analyze differences between calculations and experiments on the actual disordered experimental structures. In order to account for the main influence of structural disorder, we phenomenologically introduce inhomogeneous broadening. Furthermore, the comparison of theoretical and experimental gain spectra provides further verification of the alloy compositions and quantum well widths.

Measurements were performed using the Hakki–Paoli method on two 100 μm stripe lasers consisting of 6 nm $Ga_{1-y}In_yN_xAs_{1-x}$ single quantum well structures with 11.5 nm GaAs barriers surrounded by an AlGaAs/GaAsP/GaAs heterostructure designed for electron capture. The heterostructure gives a confinement factor of 1.8%. The chemical composition has been determined by high-resolution x-ray diffraction. For the first sample $y=42\%$ and no nitrogen, for the second sample $y=40\%$, $x=0.43\%$. Spectra of the LWEF were measured from amplified spontaneous emission below threshold at 20 °C for several currents.[17]

We compare the laser properties of GaInNAs to those of InGaAs based lasers, performing comparisons between different samples. The band structure including strain effects is

[a]Electronic mail: angela.thraenhardt@physik.uni-marburg.de

Downloaded 20 Jul 2011 to 128.180.137.141. Redistribution subject to AIP license or copyright; see http://apl.aip.org/about/rights_and_permissions

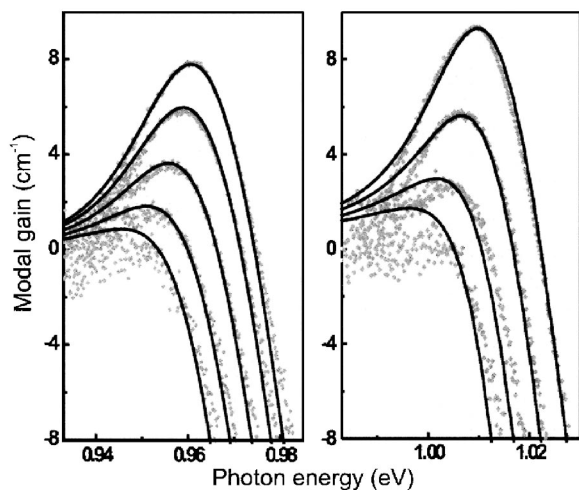

FIG. 1. (a) Calculated gain spectra for $Ga_{0.6}In_{0.4}N_{0.0043}As_{0.9957}$ and carrier densities of $1.46, 1.4, 1.31, 1.21, 1.11 \times 10^{12}/cm^2$; (b) calculated gain spectra for $In_{0.42}Ga_{0.58}As$ and carrier densities of $1.01, 0.94, 0.85, 0.77 \times 10^{12}/cm^2$. The grey dots are from experiment for injection currents of (a) 159, 180, 201, 221, and 236 mA and (b) 70, 80, 92, and 102 mA. The inhomogeneous broadening is 17 meV for GaInNAs and 11 meV for InGaAs.

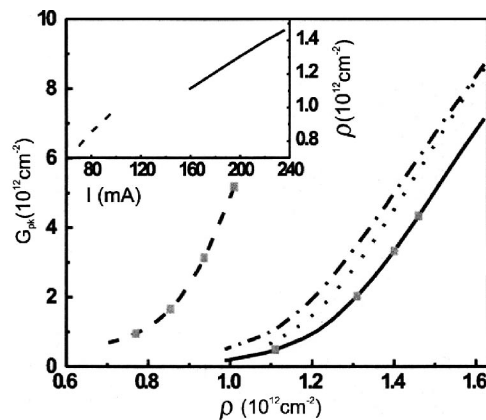

FIG. 2. Calculated peak material gain vs carrier density for $In_{0.42}Ga_{0.58}As$ (dashed) with an inhomogeneous broadening of 11 meV, $Ga_{0.6}In_{0.4}N_{0.0043}As_{0.9957}$ with an inhomogeneous broadening of 17 meV (solid) and for predominantly homogeneous broadening for $Ga_{0.6}In_{0.4}N_{0.0043}As_{0.9957}$ sample (dotted) and $Ga_{0.6}In_{0.4}N_{0.015}As_{0.985}$ (dash–dotted). The squares are experimental values. We observe excellent agreement between theory and experiment. Inclusion of nitrogen lowers the slope of the curve, i.e., the differential gain. The inset shows the conversion of experimental injection currents to ρ for GaInNAs (solid) and InGaAs (dashed) samples as obtained from Fig. 1.

computed in a 10×10 $\mathbf{k}\cdot\mathbf{p}$ model, incorporating an anticrossing model for the inclusion of nitrogen.[18,19] The optical susceptibility is then calculated by way of the semiconductor Bloch equations treating Coulomb correlations at the second Born and Markov level[20,21] and taking into account carrier–carrier and carrier–LO phonon scattering which are the relevant scattering processes at room temperature. Disorder effects from alloy or local well width fluctuations are modeled by a Gaussian broadening of the gain spectra. The theory has already been shown to well reproduce optical properties of various heterostructures, including those in the GaInNAs material system.[9,17,22,23] As input for the current study, we only need basic band structure parameters which are listed in Ref. 23.

Figure 1 shows a comparison of calculated and measured gain spectra for the (a) GaInNAs and (b) InGaAs sample. Note that the dephasing rate is not treated as a free parameter in the calculations, but is the result of microscopic calculation. We observe good agreement between theory and experiment, using carrier density and inhomogeneous broadening linewidth as the only fit parameters. By this means we extract the ρ in the system, which is shown in the inset of Fig. 2 as a function of the injection current. Interestingly, we observe that for a comparable change in peak gain, the density variation is much less in the N-free sample than in the GaInNAs sample.

To analyze the origin of this reduced gain variation we plot in Fig. 2 calculations of the peak gain versus ρ. The dashed line represents the InGaAs sample. It shows a much steeper slope or differential gain $G' = dG/d\rho$ than the solid line for the $x=0.43\%$ –GaInNAs sample as well as the dash–dotted line for a GaInNAs sample with an even higher N content, $x=1.5\%$, corresponding to a peak gain energy of around 0.85 eV. The inclusion of nitrogen increases the effective electron mass and moves the conduction subbands closer to each other, thus increasing the density of states. This leads to a flatter electron distribution, and consecutively to a drastic difference of the peak gain for GaInNAs and InGaAs samples. In our case the band structure induced changes of the gain dominate compared to the effects of the different inhomogeneous broadening. Now we consider the influence of increasing N content on differential gain excluding any deviation from the perfect crystal and comparing homogeneously broadened samples with $x=1.5\%$ and $x=0.43\%$. The sample with higher N content shows higher gain at low ρ and a lower differential gain. For low N concentration the energy of the N-level is closer to the conduction band edge.[24] The flattening of the conduction band for higher electron momenta provides an increased number of states and the electrons spread out into them. This effectively reduces the inversion at the band minimum, which in turn reduces the peak gain.

Figure 3 displays measured LWEF values. Experimentally, the differential gain and index of refraction were obtained by switching between currents of (a) 201 and 236 mA for the GaInNAs and (b) 80 and 102 mA for the InGaAs sample. We mimic this switching process computationally by

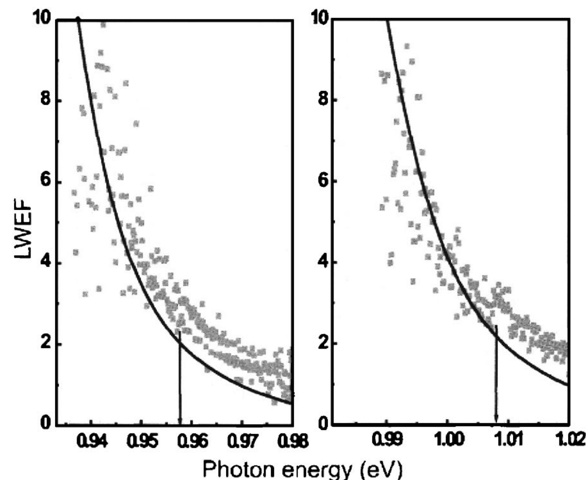

FIG. 3. LWEF for (a) $Ga_{0.6}In_{0.4}N_{0.0043}As_{0.9957}$ and (b) $In_{0.42}Ga_{0.58}As$ determined experimentally (grey squares) and theoretically (lines). The arrow indicates the position of the corresponding peak gain for injection currents of 201 and 236 mA for the GaInNAs (a) and for the InGaAs sample (b) for injection currents of 80 and 102 mA.

Downloaded 20 Jul 2011 to 128.180.137.141. Redistribution subject to AIP license or copyright; see http://apl.aip.org/about/rights_and_permissions

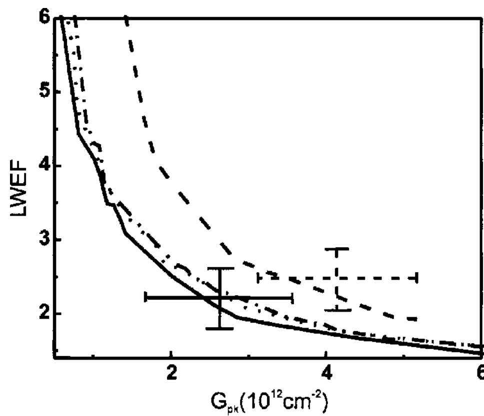

FIG. 4. LWEF at peak gain vs peak material gain for $In_{0.42}Ga_{0.58}As$ (dashed) with an inhomogeneous broadening of 11 meV, $Ga_{0.6}In_{0.4}N_{0.0043}As_{0.9957}$ with an inhomogeneous broadening of 17 meV (solid) and for predominantly homogeneous broadening for $Ga_{0.6}In_{0.4}N_{0.0043}As_{0.9957}$ sample (dotted) and $In_{0.4}Ga_{0.6}N_{0.015}As_{0.985}$ (dash–dotted). The crosses indicate the average values and error bars of the experimental gain peak alpha factor for $Ga_{0.6}In_{0.4}N_{0.0043}As_{0.9957}$ (solid) and $In_{0.42}Ga_{0.58}As$ (dashed).

using the appropriate ρ, see the inset in Fig. 2, which correspond to a variation of 10% for the density of the $x = 0.43\%$ sample. Lowering the variation of ρ to 2% decreases the computed value of the LWEF at the peak gain by a factor of 0.961, i.e., the true LWEF is somewhat overestimated experimentally because of the large variation in current.

The dashed, solid, dash–dotted and dotted lines in Fig. 4 show calculations of the LWEF for samples with $x = 0\%, 0.43\%, 1.5\%$, respectively, using a variation in density of 10% for $x=0.43\%$, 1.5%, and 16% for $x=0\%$ as in experiment. The LWEF is determined by the ratio of the carrier-induced refractive index change to the differential gain. The figure clearly shows that the inclusion of nitrogen reduces the LWEF, because of the reduction of the refractive index. The LWEF for homogeneously broadened N-containing samples show almost no difference. For comparison, we have included an inhomogeneous broadening of 17 meV for the $x=0.43\%$ case (solid line), as extracted from experiment. This leads to a slight reduction of LWEF, which is also due to a change in the refractive index. The experimental value is somewhat higher than the theoretical one, an effect which on the basis of an earlier study[9] we attribute to a nonequilibrium distribution of carriers, i.e., as a consequence of the injection pumping and the gradual relaxation the barrier states are occupied more than they would be in true thermal equilibrium.

Note that the lower differential gain in GaInNAs does not translate into a higher LWEF. In fact, both theory and experiment predict similar LWEF for the GaInNAs and InGaAs. The balancing effects of the differential gain reduction and the differential refractive index reduction maintain the LWEF basically unchanged for samples with different N content.

In summary, we investigate gain and LWEF of GaInNAs structures, comparing measurements to microscopic calculations, which show a good agreement. The LWEF is thus lowered in GaInNAs compared to InGaAs, but hardly depends on the N content of the GaInNAs sample.

This work was supported by the Deutsche Forschungsgemeinschaft (Research Group on Metastable Compound Semiconductors and Heterostructures), by AFOSR (F49620-02-1-0380 and FA9550-04-1-0372), the U.S. Department of Energy (DE-AC04-94AL8500) and the Senior Scientist Award and the Max-Planck Research Prize of the Max-Planck Society and Humboldt Foundation.

[1] Semicond. Sci. Technol. **17**, special issue: III–N–V Semiconductor Alloys (2002).
[2] IEE Proc.: Optoelectron. **150**, special issue: Physics and Technology of Dilute Nitrides for Optical Communications (2003).
[3] J. Phys.: Condens. Matter **16**, special issue: Articles on Dilute Nitrides (2004).
[4] W. W. Chow, K. D. Choquette, M. H. Crawford, K. L. Lear, and G. R. Hadley, IEEE J. Quantum Electron. **33**, 1810 (1997).
[5] N. C. Gerhardt and M. R. Hofmann, J. Phys.: Condens. Matter **16**, S3095 (2004).
[6] D. Alexandropoulos and M. J. Adams, J. Phys.: Condens. Matter **14**, 3523 (2002).
[7] J. C. L. Yong, J. M. Rorison, M. Othman, H. D. Sun, M. D. Dawson, and K. A. Williams, IEE Proc.: Optoelectron. **150**, 80 (2003).
[8] H. Carrère, A. Arnoult, X. Marie, T. Amand, E. Bedel-Pereira, R. J. Potter, and N. Balkan, Physica E (Amsterdam) **17**, 245 (2003).
[9] N. C. Gerhardt, M. R. Hofmann, J. Hader, J. V. Moloney, S. W. Koch, and H. Riechert, Appl. Phys. Lett. **84**, 1 (2004).
[10] W.-H. Seo and J. F. Donegan, Appl. Phys. Lett. **82**, 505 (2003).
[11] B. Witzigmann, M. S. Hybertsen, C. L. Reynolds, G. L. Belenky, L. Shterengas, and G. E. Shtengel, IEEE J. Quantum Electron. **39**, 120 (2003).
[12] W. W. Chow, E. D. Jones, N. A. Modine, A. A. Allerman, and S. R. Kurtz, Appl. Phys. Lett. **75**, 2891 (1999).
[13] C. K. Kim and Y. H. Lee, Appl. Phys. Lett. **79**, 3038 (2001).
[14] S. Tomić and E. P. O'Reilly, IEEE Photonics Technol. Lett. **15**, 6 (2003).
[15] W. W. Chow and J. S. Harris, Jr., Appl. Phys. Lett. **82**, 1673 (2003).
[16] M. Hofmann, A. Wagner, C. Ellmers, C. Schlichenmaier, S. Schäfer, F. Höhnsdorf, J. Koch, W. Stolz, S. W. Koch, W. W. Rühle, J. Hader, J. V. Moloney, E. P. O'Reilly, B. Borchert, A. Yu. Egorov, and H. Riechert, Appl. Phys. Lett. **78**, 3009 (2001).
[17] L. Shterengas, J.-Y. Yeh, L. J. Mawst, N. Tansu, and G. Belenky, CLEO, May 16–21 (2004) San Francisco, CA, edited by Alexander A. Sawchuk.
[18] E. P. O'Reilly and A. Lindsay, Phys. Status Solidi B **216**, 131 (1999).
[19] A. Lindsay and E. P. O'Reilly, Solid State Commun. **112**, 443 (1999).
[20] A. Girndt, F. Jahnke, A. Knorr, S. W. Koch, and W. W. Chow, Phys. Status Solidi B **202**, 725 (1997).
[21] J. Hader, J. V. Moloney, and S. W. Koch, IEEE J. Quantum Electron. **35**, 1947 (1999).
[22] J. Hader, S. W. Koch, J. V. Moloney, and E. P. O'Reilly, Appl. Phys. Lett. **76**, 3685 (2000).
[23] J. Hader, S. W. Koch, and J. V. Moloney, Solid-State Electron. **47**, 513 (2003).
[24] S. Tomić, E. P. O'Reilly, P. J. Klar, H. Grüning, W. Heimbrodt, W. M. Chen, and I. A. Buyanova, Phys. Rev. B **69**, 245305 (2004).

Downloaded 20 Jul 2011 to 128.180.137.141. Redistribution subject to AIP license or copyright; see http://apl.aip.org/about/rights_and_permissions